Structural Studies of a Complex between endothelial Nitric Oxide Synthase and Calmodulin at Physiological Calcium Concentration

Michael Piazza, Thorsten Dieckmann and J. Guy Guillemette*[1,*]

Department of Chemistry, University of Waterloo, Waterloo, Ontario N2L 3G1, Canada

[1] This work was supported, in whole or in part, by the Natural Sciences and Engineering Research Council of Canada (NSERC) via Grants 326911 (to T.D) and 183521 (to J.G.G)

[*] To whom correspondence should be addressed: Dept. of Chemistry, University of Waterloo, 200 University Ave. W, Waterloo, Ontario N2L 3G1 Canada. Tel. 519-888-4567 ext. 35954; Fax 519-746-0435; E-mail: jguillem@uwaterloo.ca; tdieckma@uwaterloo.ca

Abbreviations: NOS, nitric oxide synthase; iNOS, inducible NOS; eNOS, endothelial NOS; nNOS, neuronal NOS; CaM, Calmodulin; NMR, nuclear magnetic resonance; CaM-eNOS complex, CaM-eNOS binding domain peptide in complex; PDB, Protein Data Bank; HSQC, heteronuclear single-quantum coherence; apoCaM, Ca^{2+} deplete CaM; PELDOR, pulsed electron-electron double resonance; FRET, fluorescence resonance energy transfer; EM, electron cryo-microscopy; SPR, surface plasmon resonance; CaM_{12}, CaM protein defective in Ca^{2+} binding in the N-lobe EF hands with CaM D20A and D56A mutations; CaM_{34}, CaM protein defective in Ca^{2+} binding in the C-lobe EF hands with CaM D93A and D129A mutations; r.m.s.d., root-mean-square distance; H/D, hydrogen/deuterium.

ABSTRACT: The small acidic protein Calmodulin (CaM) serves as a Ca^{2+} sensor and control element for many enzymes including nitric oxide synthase (NOS) enzymes that play major roles in key physiological and pathological processes. CaM binding causes a conformational change in NOS to allow for the electron transfer between the reductase and oxygenase domains through a process that is thought to be highly dynamic. In this report, NMR spectroscopy was used to determine the solution structure of the endothelial NOS (eNOS) peptide in complex with CaM at the lowest Ca^{2+} concentration (225 nM) required for CaM to bind to eNOS and corresponds to a physiological elevated Ca^{2+} level found in mammalian cells. Under these conditions, the CaM-eNOS complex has a Ca^{2+}-replete C-terminal lobe bound the eNOS peptide and a Ca^{2+} free N-terminal lobe loosely associated to the eNOS peptide. With increasing Ca^{2+} concentration, the binding of Ca^{2+} by the N-lobe of CaM results in a stronger interaction with the C-terminal region of the eNOS peptide and increased α-helical structure of the peptide that may be part of the mechanism resulting in electron transfer from the FMN to the heme in the oxygenase domain of the enzyme. SPR studies performed under the same conditions show Ca^{2+} concentration dependent binding kinetics were consistent with the NMR structural results. This investigation shows that structural studies performed under more physiological relevant conditions provide information on subtle changes in structure that may not be apparent when experiments are performed in excess Ca^{2+} concentrations.

Calmodulin (CaM) is a small cytosolic Ca^{2+}-binding protein that is able to bind and regulate hundreds of different intracellular proteins.[1] CaM consists of two globular domains connected by a flexible central linker region. Each globular domain contains two EF hand pairs that are capable of binding to Ca^{2+}. Upon binding of Ca^{2+} to the EF hands of CaM, CaM undergoes a conformational change that exposes hydrophobic patches on each domain that allow CaM to associate with its intracellular target proteins. The binding of Ca^{2+} to CaM is cooperative within each lobe of CaM but not between the lobes, with the C-lobe of CaM able to bind Ca^{2+} with a ten-fold higher affinity than the N-lobe.[2,3] The flexibility of the central linker connecting the N- and C-lobes of CaM allows it to adapt its conformation to optimally associate with its intracellular targets.[4]

The target proteins bound and regulated by CaM include the nitric oxide synthase (NOS) enzymes, which catalyze the production of nitric oxide (•NO).[5] There are three NOS isoforms in mammals: neuronal NOS (nNOS), endothelial NOS (eNOS), and inducible NOS (iNOS). All are all dimers, with each monomer containing an N-terminal oxygenase domain and a C-terminal reductase domain, connected by a CaM binding domain. The CaM binding domains of NOS contain the classical 1-5-8-14 CaM-binding motif. CaM is found to bind to this binding domain in an antiparallel fashion, with the N-lobe of CaM binding closer to the C-terminus of this domain, and the C-lobe of CaM binds closer to the N-terminus.[6] CaM's interaction with eNOS and nNOS is Ca^{2+}-dependent, requiring 200-300 nM concentrations of free Ca^{2+} to achieve half maximal activity,[7,8] whereas CaM binds to iNOS regardless of intracellular Ca^{2+} concentration and is fully active at basal levels of Ca^{2+} (<100 nM) in the cell.[9–12] The oxygenase domain contains binding sites for heme, tetrahydrobiopterin (H_4B), and the substrate L-arginine. The reductase domain contains binding sites for the cofactors FMN, FAD, and NADPH.[5,13]

Electron flow in the NOS enzymes occurs from the NADPH, through the FAD and FMN cofactors, to the heme oxygenase domain. Recent studies using pulsed electron-electron double resonance (PELDOR)

spectroscopy, single-molecule fluorescence resonance energy transfer (FRET) spectroscopy, and electron cryo-microscopy (EM) have given better insight into the CaM activated NOS mechanism.[14–19] These studies show the NOS enzymes consist of a dimerized oxygenase domain that acts as the anchoring dimeric structure for the entire enzyme molecule. This is flanked by two separated reductase domains, that exist in an equilibrium of conformations that alternate between FAD-FMN electron transfer (input state) and FMN–heme electron transfer (output state) with CaM binding inducing a shift in the conformational equilibrium to allow efficient electron transfer in NOS enzymes. When CaM is fully bound to NOS, residues of CaM's N-lobe interact with the FMN subdomain of NOS and form a bridge interaction that appears necessary to control the interaction between the FMN and heme.[20] CaM activates NOS through the stabilization and precise positioning of the FMN subdomain for the shuttling of electrons from the FMN to the oxygenase domain.

CaM's interactions with the various NOS isoforms has previously been studied by surface plasmon resonance (SPR) and nuclear magnetic resonance (NMR).[21–26] However, most structural and dynamics studies on CaM-NOS interactions have been performed at non-physiological conditions using either apo (Ca^{2+} free with excess chelators, such as EDTA, present) or Ca^{2+} saturated (greater than 1mM Ca^{2+}) conditions which don't represent the true intracellular Ca^{2+} concentration. Previously, we had determined the minimal free Ca^{2+} concentration needed for CaM to interact with eNOS to be 225 nM.[27] In the present study we determined the binding kinetics and NMR structure of CaM bound to the human eNOS CaM binding domain peptide (CaM−eNOS complex) at a free Ca^{2+} concentration that represents this elevated intracellular Ca^{2+} concentration of 225 nM. A comparison was made with the less physiologically relevant high Ca^{2+} concentrations used in previous CaM-eNOS structure calculations. Our study is the first study to determine a solution structure of the CaM-eNOS complex at a free Ca^{2+} concentration that is in the

elevated intracellular Ca^{2+} concentration range. In addition, this study identifies the roles played by each individual lobe of CaM in the binding and activation of the eNOS enzyme.

EXPERIMENTAL PROCEDURES

CaM Protein Expression and Purification. Wild-type CaM protein, CaM_{12} (CaM protein defective in Ca^{2+} binding in the N-lobe EF hands; CaM D20A and D56A mutations) and CaM_{34} (CaM protein defective in Ca^{2+} binding in the C-lobe EF hands; CaM D93A and D129A mutations) were expressed and purified using phenyl sepharose chromatography, as previously described.[28] Isolation of the CaM protein (148 residues) was confirmed by ESI-MS and purity was judged to be > 95% by SDS-PAGE. The human eNOS (TRKKTFKEVANAVKISASLMGT, 22 residues corresponding to residues 491-512 from the full length eNOS protein) peptide was synthesized and purchased from Sigma. The eNOS peptide used for SPR was synthesized with an added cysteine at the carboxyl end to allow for immobilization on the gold sensor.

Sample Preparation for NMR Investigation. CaM for NMR experiments was expressed in E. coli in M9 media (11.03 g/L $Na_2HPO_4 \cdot 7H_2O$, 3.0 g/L KH_2PO_4, 0.5 g/L NaCl, 2 mM $MgSO_4$, 0.1 mM $CaCl_2$, 5 mg/mL Thiamine, 100 μg/mL kanamycin) containing 2 g/L ^{13}C-glucose and 1 g/L $^{15}NH_4Cl$.[22] ^{13}C-^{15}N-CaM was purified using phenyl sepharose chromatography, as previously described.[28] Isolation of the CaM protein (148 residues) was confirmed by ESI-MS and purity was judged to be > 95% by SDS-PAGE.

The 225 nM free Ca^{2+} ^{13}C-^{15}N-CaM sample was prepared via a buffer exchange into 30 mM MOPS, 100 mM KCl, 90% H_2O/10% ^2H_2O, pH 7.2, and combination of 10 mM EGTA and 10mM CaEGTA to obtain a final 225 nM concentration of free Ca^{2+} using a YM10 centrifugal filter device (Millipore Corp., Billerica, USA). The sample had a final ^{13}C-^{15}N-CaM concentration of 1 mM in a total volume of 500 μL. The sample was transferred into 5 mm NMR sample tubes and stored at 4^{o}C until required for NMR experiments. NMR experiments on the complex were conducted on samples titrated with eNOS peptide to saturation in a 1:1 CaM:peptide ratio. The eNOS peptide was run through a Chelex exchange resin prior

to lyophilization for the NMR titrations. Complex formation was monitored after each addition by acquisition of a ^{1}H-^{15}N heteronuclear single-quantum coherence (HSQC) spectrum.

NMR Spectroscopy and Data Analysis. NMR spectra were recorded at 25°C on Bruker 600 MHz DRX spectrometers equipped with XYZ-gradients triple-resonance probes (Bruker, Billerica, MA, USA). Spectra were analyzed using the program CARA (Computer Aided Resonance Assignment).[29] The amide resonances assignments were aided by using the previously obtained amide chemical shifts of Ca^{2+} saturated CaM with eNOS peptide as reference.[22] Specific assignments of the backbone resonances were achieved using a combination of three-dimensional triple- resonance experiments, including HNCA, HN(CO)CA, CBCA(CO)NH, and HNCO.[30–32] Side chain resonances were assigned using the TOCSY-type HC(C)H-TOCSY and (H)CCH- TOCSY experiments.[33]

Structure Calculation of CaM-eNOS Peptide at 225 nM Ca^{2+}. The ^{1}H, ^{13}C, and ^{15}N resonance assignments were utilized to identify constraints for the structure calculations. Distance constraints for the CaM-eNOS complex were obtained from ^{15}N NOESY-HSQC and ^{13}C NOESY- HSQC, and ^{15}N- double-filtered NOESY spectra acquired on samples containing ^{13}C-^{15}N-CaM and unlabeled peptide.[34–36] In addition, dihedral angle restraints were derived from chemical shift analysis with TALOS+. The structure calculation of CaM-eNOS peptide at 225 nM Ca^{2+} was performed using CNSsolve version 1.2.[37] The calculation was initiated with an extended conformation file and run through several iterations of a standard simulated annealing protocol to minimize the energies. The final 20 lowest energy structures were selected.

Accession Numbers. The coordinates and NMR parameters have been deposited in the Protein Data Bank (PDB) and the BioMagResBank (BMRB) and have been assigned PDB entry 2N8J, and BMRB accession number 25852.

Surface Plasmon Resonance. SPR experiments were performed with an openSPR instrument (Nicoya Lifesciences, Waterloo, Canada) at 25°C with a 100 μL loading loop and a constant flow rate of 50 μL/min. The eNOS peptide with an added cysteine at the carboxyl end was immobilized on a gold nanoparticle sensor chip. Binding of CaM was tested in either saturating Ca^{2+} buffer (30 mM MOPS, 100 mM KCl, pH 7.2 and 0.1 mM $CaCl_2$) or 225 nM free Ca^{2+} buffer (30 mM MOPS, 100 mM KCl, pH 7.2, and combination of 10 mM EGTA and 10mM CaEGTA to obtain a final 225 nM concentration of free Ca^{2+}). CaM was injected over the immobilized eNOS peptide in concentrations from 10 to 500 nM for 2 minutes to allow association. CaM free saturating Ca^{2+} or 225 nM free Ca^{2+} buffer was passed over the sensor for 12 minutes to allow dissociation. Following each CaM injection, 30 mM MOPS, 100 mM KCl, pH 7.2 and 10 mM EDTA buffer was injected to completely dissociate the complex and regenerate the sensor. Analysis of the data was made using Trace Drawer software (Ridgeview Instruments AB) as recommended by the manufacturer. Kinetic parameters were calculated using global analysis, fitting the data to a simple 1:1 model ($A + B \leftrightarrow AB$) for CaM-, CaM_{12}- and CaM_{34}- interactions at saturated and 225 nM Ca^{2+}.

RESULTS AND DISCUSSION

NMR experiments were performed at physiological free Ca^{2+} concentrations to provide further insights into the structural differences and dynamics of the CaM-eNOS complex. These results were compared to the non-physiological high Ca^{2+} concentrations used in past CaM-NOS structure calculations.[22,38,39] At resting intracellular Ca^{2+} concentrations CaM is unable to bind to the eNOS CaM binding domain peptide, whereas it can bind at an elevated free Ca^{2+} concentration of 225 nM. At the 225 nM free Ca^{2+} concentration CaM alone does not bind Ca^{2+} (previously shown by dansyl-CaM fluorescence studies [27]), however, the presence of the eNOS peptide enhances the Ca^{2+} affinity of the C-lobe of CaM. At resting

intracellular Ca^{2+} concentrations holo eNOS is also inactive, requiring a 200 to 300 nM free Ca^{2+} concentration to achieve half maximal activity.[8,40–43]

NMR Structure at Physiological Ca^{2+} Concentration. The three-dimensional solution structure of CaM bound to the human eNOS CaM binding domain peptide (CaM−eNOS complex) at 225 nM free Ca^{2+} was determined using multidimensional heteronuclear NMR spectroscopy. The structure of the complex is based on a large number of experimental constraints and is well-defined. The root-mean-square distance (r.m.s.d.) for ordered residues is 1.9 Å for the backbone atoms and 2.2 Å for all non-hydrogen atoms (Table 1). The family of 20 lowest energy structures is shown in Fig. 1A. When these 20 lowest energy structures are aligned by the C-lobe backbone atoms of CaM, the C-lobes of CaM are shown to superimpose quite well with each other, whereas the N-lobe has a lot of fluctuation in its relative position to the C-lobe, suggesting the N-lobe is less rigid, and more dynamic, than the C-lobe. When a similar comparison is made with the superposition of the backbone of the 20 lowest energy structures for the previously determined Ca^{2+} saturated CaM-eNOS complex (PDB 2LL7, Fig. 1D) both the C- and N-lobes display fairly rigid and well overlaid structures. This less rigid, or more dynamic, N-lobe of CaM in the CaM-eNOS complex structure at 225 nM free Ca^{2+} can also be shown by looking at the r.m.s.d. values for each individual lobe of CaM. The r.m.s.d. for the C-lobe residues is 0.6 Å for the backbone atoms and 1.1 Å for all non-hydrogen atoms, whereas it is 0.9 Å for the backbone atoms and 1.4 Å for all non-hydrogen atoms of the N-lobe.

The CaM-eNOS complex at a physiologically relevant free Ca^{2+} concentration of 225 nM has a Ca^{2+}-replete C-lobe bound to the eNOS peptide and a Ca^{2+} free N-lobe loosely associated to the eNOS peptide in an antiparallel fashion as shown in Fig. 1B. Residues 1−4 (corresponding to residues 491−494 of eNOS) at the N-terminus of the eNOS CaM-binding region peptide show a lack of structure because they could

not be unambiguously assigned. Compared to the Ca^{2+} saturated CaM-eNOS complex structure (Fig. 1E) one can see that the N-lobe at 225 nM free Ca^{2+} has a much looser association to the eNOS peptide.

The Solution Structure of CaM-eNOS at 225 nM Free Ca^{2+} Correlates Well with Previous Dynamics Data. The dynamic properties of these complexes had been previously examined by amide H/D exchange time-course and NMR ^{15}N relaxation experiments and agree very well with the determined solution structure in this study.[27] Amide exchange experiments provide detailed information on the degree of protection of specific residues within a protein complex and are useful for identifying residues involved in co-operative binding of a ligand.[44,45] The NMR ^{15}N relaxation T_1, T_2, and ^1H-^{15}N NOE experiments were used to characterize backbone mobility by determining an order parameter, S^2, which may be interpreted to describe internal dynamics on a residue specific level.[46–49] There are a few residues of the N-lobe that exhibit intermediate exchange, such as M36, M51, M72 and K75. These residues are all found to be part of α-helices and have hydrophobic interactions with L509, one of the anchoring residues of eNOS, in the solution structure of the complex (Fig. 1C and fig. 3C). The amides of the C-lobe residues that show intermediate or slow exchange correspond to CaM residues that also interact with the 1-5-8-14 anchoring residues of the eNOS peptide in the solution structure (Fig. 3B). The ^{15}N relaxation data also correlates very well with the solution structure of the CaM-eNOS complex at 225 nM Ca^{2+}. The lower overall dynamics of the C-lobe of CaM compared to the N-lobe correspond well with the more rigid C-lobe (and lower r.m.s.d. for the C-lobe) observed in the structure. Whereas the N-lobe of CaM displays increased backbone mobility, indicating increased dynamics, which correlates well with the less rigid N-lobe observed by the increased fluctuations in its overall position relative to the C-lobe (Fig. 1A) and the N-lobe's higher calculated r.m.s.d. value.

This provides direct structural evidence for previous studies that show CaM bound to the NOS holoenzymes exists in multiple conformations with the most populated state corresponding to CaM docked

to the oxygenase domain (CaM binds to the oxygenase domain with its C-lobe).[14–19] The more highly dynamic N-lobe of CaM (which interacts with the FMN subdomain of eNOS) is consistent with the proposed conformational sampling of the FMN subdomain.[14,15]

Comparison to Previous CaM Structures. When the 225 nM free Ca^{2+} CaM-eNOS complex structure is compared to the previously determined Ca^{2+} saturated CaM−eNOS complex structure (PDB entry 2LL7), one can see that the C-lobes of CaM and peptide orientation are quite similar, however the N-lobe of CaM is structurally different (Fig. 2A,B). When the two structures are aligned with respect to CaM's C-lobe backbone atoms a r.m.s.d. value of 1.023 Å for the backbone atoms of CaM was found. The C-lobes of CaM and the eNOS peptide of each structure superimpose quite well on each other, whereas the N-lobes of CaM do not.

When the 225 nM free Ca^{2+} CaM-eNOS complex structure is compared to the previously determined apoCaM structure (PDB entry 1CFC), there is structural similarity of the N-lobes of CaM, whereas the C-lobes of CaM show differences (Fig. 2C,D). When the two structures are aligned with respect to CaM's N-lobe backbone atoms a r.m.s.d. value of 1.042 Å for the backbone atoms of CaM was found.

The Individual Lobes of CaM Interact Differently With the eNOS Peptide at Low Ca^{2+} Concentrations. At the 225 nM free Ca^{2+} concentration the CaM-eNOS complex displays a structure with a Ca^{2+}-replete C-lobe bound to the peptide, and a Ca^{2+}-deplete N-lobe that is loosely associated to the peptide via hydrophobic interactions of a few CaM residues to the anchoring residue L509 of eNOS (Fig 3A,C). The solution structure shows L509 situated in a hydrophobic pocket of CaM composed of N-lobe residues M36, M51, and M72.

The structure of the CaM-eNOS complex at 225 nM Ca^{2+} shows that the C-lobe of CaM is completely bound to the N-terminal region of the eNOS peptide in a similar fashion as the holoCaM-eNOS complex. Residues V91, F92, L105, L112, F141 and M144 of the C-lobe of CaM interact via hydrophobic

interactions with the anchoring residues F496, A500 and V503 of the eNOS peptide (Fig 3A, B). This forms a tight complex between the eNOS peptide and CaM which induces this region of the eNOS peptide to adopt an α-helical secondary structure. The C-terminus of the eNOS peptide does not form an α-helix likely due to having weaker interactions with the N-lobe of CaM. This is evidenced by the solution structure and the lower amount of NOE contacts observed in the eNOS peptide NOESY spectrum and agrees very well with previous studies that show the NOS peptides have no secondary structure when not bound to CaM.[21,50] This less structured C-terminal region of the eNOS CaM binding domain supports a weaker association of the N-lobe of CaM to the eNOS peptide and would allow the FMN subdomain to have the flexibility to sample different conformational states, correlating well with the dynamic nature of this region of the NOS enzyme.

The solution structure, along with the previous amide exchange and internal mobility results, show that the residues of CaM interacting with eNOS' 1-5-8-14 anchoring residues have a strong interaction at 225 nM free Ca^{2+} concentration, which keeps the complex bound, while the rest of the residues of the CaM protein are able to fluctuate or "breathe". Comparing the two lobes of CaM, the residues of the C-lobe display a more rigid structure (lower r.m.s.d., lower degree of internal mobility (higher S^2) and higher exchange protection), indicating a stronger interaction with the N-terminal region of the eNOS peptide to hold the complex together and induce an α-helical structure, while the N-lobe is more dynamic and loosely associated to the less structured C-terminal region of the eNOS peptide. This further supports a previous study of CaM with a NOS isoform that showed the C-lobe of CaM first binds Ca^{2+}, then to the nNOS enzyme, followed by an increase in intracellular Ca^{2+} concentration where the N-lobe is then able to bind Ca^{2+} and finally to the enzyme.[51]

Surface Plasmon Resonance Show Increase in Ca^{2+} Concentration Stabilizes the CaM-eNOS Complex. The interaction of the eNOS peptide with CaM at 225 nM Ca^{2+} was further analyzed using

SPR. SPR analysis allows us to determine the binding kinetics of a protein to a peptide with the advantage of using a label-free system. The kinetics of this binding interaction, including the binding affinity, association and dissociation rates, was determined by the injection of different concentrations of CaM over a surface with an immobilized eNOS peptide.

Sensorgrams at various CaM concentrations (10 to 500 nM) were obtained at a saturating Ca^{2+} concentration of 0.1 mM to ensure optimal interaction of Ca^{2+}-replete CaM with the eNOS peptide (Figure 4). The sensorgrams consisted of three phases: an association phase, injection of buffer with CaM; a dissociation phase, flushing of the flow cell with CaM-free buffer; and a regeneration phase, injection of EDTA for complete dissociation of the complex. Sensorgrams were analyzed by a simple 1:1 ($A + B \leftrightarrow AB$, where A is CaM and B is the immobilized eNOS peptide) fitting model using the Tracedrawer software (Ridgeview Instruments AB) (Figure 4 and Table 2).

We determined the association rate, k_a, to be 13.1 (± 4.84) x 10^4 $M^{-1}s^{-1}$ and the dissociation rate, k_d, to be 3.47 (± 1.03) x 10^{-4} s^{-1}, giving a dissociation constant, K_D, of 2.68 (± 0.17) x 10^{-9} M for CaM at saturating Ca^{2+}, which is in good agreement with previously reported values that range from 1.6 to 4.0 x 10^{-9} M.[21,52,53] Sensorgrams were then obtained at the 225 nM free Ca^{2+} concentration to evaluate the initial binding kinetics of CaM with the eNOS peptide. This yielded a k_a of 7.79 (± 0.47) x 10^4 $M^{-1}s^{-1}$, k_d of 8.33 (± 0.72) x 10^{-4} s^{-1} and K_D of 10.7 (± 0.28) x 10^{-9} M.

To evaluate the binding kinetics of each individual Ca^{2+} saturated lobe of CaM to the eNOS peptide we performed SPR experiments at either saturating (0.1 mM $CaCl_2$) or 225 nM free Ca^{2+} concentration using CaM constructs that are defective in Ca^{2+} binding in either the N-terminal lobe EF hands (CaM_{12}; CaM D20A and D56A mutations) or the C-terminal lobe EF hands (CaM_{34}; CaM D93A and D129A). The CaM_{12} construct is only able to bind Ca^{2+} to the C-lobe of CaM which resembles the conformation of wildtype CaM with the eNOS peptide at 225 nM free Ca^{2+}. The SPR analysis showed for saturating and

225 nM free Ca^{2+} conditions CaM_{12} had similar binding kinetics to the eNOS peptide (K_D's of 14.4 ± 4.0 and 18.0 ± 2.7 nM, respectively and increased dissociation rates) as wildtype CaM with the peptide at 225 nM free Ca^{2+}. The SPR experiment with the CaM_{34} construct allows us to measure the contribution of the N-lobe of CaM to the binding kinetics with the eNOS peptide. The interaction of eNOS with CaM is Ca^{2+}-dependent, thus CaM is unable to associate with eNOS in its Ca^{2+} free form. The binding of CaM_{34} to the eNOS peptide was found to be very weak at 225 nM free Ca^{2+} (data not shown) because the C-lobe of CaM is incapable of binding Ca^{2+} and at this low Ca^{2+} concentration the N-lobe of CaM is unable to bind Ca^{2+} in the presence of the peptide as shown by the NMR data. At saturated Ca^{2+} CaM_{34} binds the eNOS peptide with the highest K_D (22.7 ± 1.0 nM) revealing that when CaM only has a Ca^{2+} saturated N-lobe it has a weaker association with the peptide, showing that the C-lobe of CaM is primarily responsible for binding to eNOS with N-lobe binding enhancing the interaction. A comparison of the different conditions and constructs used in the investigation shows that a correlation exists between the binding kinetics and constants (Figure 5). When only one lobe of CaM is able to interact with the eNOS peptide, the dissociation rates and dissociation constants are increased when compared to CaM binding the eNOS peptide at saturated Ca^{2+}.

At 225 nM free Ca^{2+} CaM's binding affinity for eNOS is decreased (increased dissociation rate) compared to the saturating Ca^{2+} conditions due to having a Ca^{2+} saturated C-lobe tightly bound to the eNOS peptide, while the N-lobe is loosely associated. At this low Ca^{2+} concentration CaM is found to be in the apo form, however, the presence of the eNOS peptide enhances CaM's C-lobe affinity for Ca^{2+} allowing it to interact and bind to the peptide.[21,27,43] The macroscopic Ca^{2+} binding constants for CaM in the absence and presence of the eNOS peptide have previously been determined and showed the addition of eNOS peptide drastically increased CaM's affinity of Ca^{2+} ($\log K_1K_2$ and $\log K_3K_4$ of 11.9 and 10.5 for CaM alone and 14.4 and 14.1 for CaM with eNOS).[21] The slower association rate can be attributed to the

C-lobe of CaM undergoing a conformation change to the Ca^{2+}-replete form while also binding to the peptide, and the N-lobe of CaM weakly interacting with the peptide in the Ca^{2+}-deplete form. In contrast, at the saturated Ca^{2+} concentration CaM is already in the Ca^{2+}-replete conformation with both lobes binding simultaneously to the peptide. The increased dissociation rate at the low Ca^{2+} concentration results from the fast dissociation of the loosely bound N-lobe followed by dissociation of the tightly bound C-lobe, while at saturated Ca^{2+} the two tightly bound lobes of CaM are required to dissociate. A 1:1 (two state) conformation change model ($A + B \leftrightarrow AB \leftrightarrow AB^*$) in which, the C-lobe of CaM binds the peptide to form the initial complex, AB, then the conformation of the complex is altered upon the loose association of the N-lobe, AB*, may be more suitable to describe this interaction. This type of fitting model has been previously used to fit sensorgram data for various CaM-target peptide interactions. [43,54–56] When the sensorgrams were fit using this model (Figure S1 and Table S1) the apparent K_D values determined were quite similar to the K_D values obtained using the simple fit model.

The association and dissociation of CaM_{12} with eNOS at 225 nM Ca^{2+} can also be described by this low Ca^{2+} binding rationale, while at saturated Ca^{2+} the higher association rate is due to the lack of conformational change required by CaM_{12}'s C-lobe (already Ca^{2+}-replete at this Ca^{2+} concentration) before association with the peptide. CaM_{34}'s weak binding to the eNOS peptide at 225 nM free Ca^{2+} shows that at this Ca^{2+} concentration the N-lobe is unable to bind Ca^{2+} in the presence of the peptide and thus CaM is unable to associate with the eNOS peptide (C-lobe of CaM is incapable of binding Ca^{2+}). CaM_{12}'s lower K_D compared to CaM_{34}'s shows when CaM only has a Ca^{2+} saturated N-lobe it has weaker binding with the peptide, whereas the C-lobe of CaM has increased binding affinity for the eNOS peptide.

This SPR data helps us understand the different binding kinetics of CaM interacting with NOS during various intracellular Ca^{2+} signaling events, which may allow us to further understand the activation of NOS. Binding of CaM to eNOS at an initial increased intracellular Ca^{2+} concentration of 225 nM has a

decreased association rate compared to CaM binding eNOS at a saturating Ca^{2+} concentration, due to only the tight association of the C-lobe of CaM (instead of both lobes) to eNOS. The increase in the Ca^{2+} concentration allows the N-lobe of CaM to become Ca^{2+}-replete and then bind to eNOS, resulting in a roughly threefold increase in binding affinity due to a decrease of the dissociation rate of the complex. Taking this all together the C-lobe of CaM is primarily responsible for the strong binding to the eNOS peptide, with the N-lobe enhancing this affinity, as has been proposed in other CaM studies.[57]

This is the first study to determine an NMR structure of the CaM-eNOS complex at a free Ca^{2+} concentration that is a physiologically relevant elevated intracellular Ca^{2+} concentration. The structure and SPR data suggest that when the intracellular Ca^{2+} concentration is elevated to 225 nM the C-lobe of CaM first binds Ca^{2+} and to the N-terminus of eNOS' CaM-binding domain, possibly along with part of the heme domain (which doesn't shift during electron transfer), while the N-lobe of CaM is loosely associated to the C-terminus of eNOS' CaM-binding domain and the FMN subdomain. In this dynamic state the less structured C-terminal region of the eNOS CaM binding domain would allow the FMN subdomain to have the flexibility to exist in a complex distribution of conformational states, correlating well with the dynamic N-lobe of CaM observed at 225 nM Ca^{2+}. An increase in the intracellular Ca^{2+} concentration would result in the N-lobe of CaM binding Ca^{2+} and becoming tightly bound to the C-terminus of eNOS' CaM-binding domain. This would induce α-helical structure and alter the conformational state of the FMN subdomain, allowing for the possibility of a bridge to form between CaM and the FMN subdomain as observed in the crystal structure of CaM with the FMN subdomain and CaM binding domain of iNOS.[39] This increased α-helical structure may be part of the triggering mechanism that restricts the movement of the FMN subdomain to conformations that allow for efficient electron transfer from the FMN to the heme. Our study provides a new structural insight into how CaM restricts

and regulates the dynamic conformational changes of the highly flexible FMN subdomain to allow for efficient electron transfer between the reductase and oxygenase domains.

ACKNOWLEDGEMENTS

The authors would like to thank John Dick from Nicoya Lifesciences for valuable discussions about our SPR results. Molecular graphics images were produced using the UCSF Chimera package from the Resource for Biocomputing, Visualization, and Informatics at the University of California, San Francisco.

SUPPORTING INFORMATION

k_{on} and k_{off} rate constants of eNOS target peptide to CaM at 225 nM Ca^{2+} and sat Ca^{2+}, SPR sensorgrams of the binding of various CaM constructs onto immobilized eNOS peptide at saturating Ca^{2+} (0.1 mM $CaCl_2$) and 225 nM free Ca^{2+} on OpenSPR.

REFERENCES

(1) Ikura, M., and Ames, J. B. (2006) Genetic polymorphism and protein conformational plasticity in the calmodulin superfamily: two ways to promote multifunctionality. *Proc. Natl. Acad. Sci. U. S. A. 103*, 1159–1164.

(2) Linse, S., Helmersson, A., and Forsen, S. (1991) Calcium binding to calmodulin and its globular domains. *J. Biol. Chem. 266*, 8050–8054.

(3) Pedigo, S., and Shea, M. A. (1995) Discontinuous equilibrium titrations of cooperative calcium binding to calmodulin monitored by 1-D 1H-nuclear magnetic resonance spectroscopy. *Biochemistry 34*, 10676–10689.

(4) Persechini, A., and Kretsinger, R. H. (1988) The central helix of calmodulin functions as a flexible tether. *J. Biol. Chem. 263*, 12175–12178.

(5) Alderton, W. K., Cooper, C. E., and Knowles, R. G. (2001) Nitric oxide synthases: structure, function and inhibition. *Biochem. J. 357*, 593–615.

(6) Spratt, D. E., Taiakina, V., Palmer, M., and Guillemette, J. G. (2007) Differential binding of calmodulin domains to constitutive and inducible nitric oxide synthase enzymes. *Biochemistry 46*, 8288–8300.

(7) Sessas, W. C., Harrison, J. K., Barber, C. M., Zengs, D., Durieuxn, M. E., Angelo, D. D. D., and Lynchsll, K. R. (1992) Molecular cloning and expression of a cDNA encoding endothelial cell nitric oxide synthase. *J. Biol. Chem. 267*, 15274–15276.

(8) Ruan, J., Xie, Q. W., Hutchinson, N., Cho, H., Wolfe, G. C., and Nathan, C. (1996) Inducible nitric oxide synthase requires both the canonical calmodulin-binding domain and additional sequences in order to bind calmodulin and produce nitric oxide in the absence of free Ca2+. *J. Biol. Chem. 271*, 22679–22686.

(9) Busse, R., and Mulsch, A. (1990) Calcium-dependent nitric oxide synthesis in endothelial cytosol is mediated by calmodulin. *FEBS Lett. 265*, 133–136.

(10) Balligand, J.-L., Ungureanu-Longrois, D., Simmons, W. W., Pimental, D., Malinski, T. A., Kapturczak, M., Taha, Z., Lowenstein, C. J., Davidoff, A. J., Kelly, R. A., Smith, T. W., and Michel, T. (1994) Cytokine-inducible nitric oxide synthase (iNOS) expression in cardiac myocytes. Characterization and regulation of iNOS expression and detection of iNOS activity in single cardiac myocytes in vitro. *J Biol Chem 269*, 27580–27588.

(11) Carafoli, E. (1987) Intracellular calcium homeostasis. *Annu. Rev. Biochem. 56*, 395–433.

(12) Islam, S. (2012) Calcium Signaling. Spinger.

(13) Daff, S. (2010) NO synthase: structures and mechanisms. *Nitric Oxide 23*, 1–11.

(14) Leferink, N. G. H., Hay, S., Rigby, S. E. J., and Scrutton, N. S. (2014) Towards the free energy landscape for catalysis in mammalian nitric oxide synthases. *FEBS J. 282*, 3016–3029.

(15) Sobolewska-Stawiarz, A., Leferink, N. G. H., Fisher, K., Heyes, D. J., Hay, S., Rigby, S. E. J., and Scrutton, N. S. (2014) Energy landscapes and catalysis in nitric-oxide synthase. *J. Biol. Chem. 289*, 11725–11738.

(16) Campbell, M. G., Smith, B. C., Potter, C. S., Carragher, B., and Marletta, M. a. (2014) Molecular architecture of mammalian nitric oxide synthases. *Proc. Natl. Acad. Sci. U. S. A. 111*, E3614-3623.

(17) Volkmann, N., Martasek, P., Roman, L. J., Xu, X. P., Page, C., Swift, M., Hanein, D., and Masters, B. S. (2014) Holoenzyme structures of endothelial nitric oxide synthase - An allosteric role for calmodulin in pivoting the FMN domain for electron transfer. *J. Struct. Biol. 188*, 46–54.

(18) He, Y., Haque, M. M., Stuehr, D. J., and Lu, H. P. (2015) Single-molecule spectroscopy reveals how calmodulin activates NO synthase by controlling its conformational fluctuation dynamics. *Proc. Natl. Acad. Sci. U. S. A. 112*, 11835–11840.

(19) Arnett, D. C., Persechini, A., Tran, Q. K., Black, D. J., and Johnson, C. K. (2015) Fluorescence quenching studies of structure and dynamics in calmodulin-eNOS complexes. *FEBS Lett. 589*, 1173–1178.

(20) Tejero, J., Haque, M. M., Durra, D., and Stuehr, D. J. (2010) A bridging interaction allows calmodulin to activate NO synthase through a bi-modal mechanism. *J. Biol. Chem. 285*, 25941–25949.

(21) Matsubara, M., Hayashi, N., Titani, K., and Taniguchi, H. (1997) Circular dichroism and 1H NMR studies on the structures of peptides derived from the calmodulin-binding domains of inducible and endothelial nitric-oxide synthase in solution and in complex with calmodulin. *J. Biol. Chem. 272*, 23050–23056.

(22) Piazza, M., Futrega, K., Spratt, D. E., Dieckmann, T., and Guillemette, J. G. (2012) Structure and dynamics of calmodulin (CaM) bound to nitric oxide synthase peptides: Effects of a phosphomimetic caM mutation. *Biochemistry 51*, 3651–3661.

(23) Piazza, M., Taiakina, V., Guillemette, S. R., Guillemette, J. G., and Dieckmann, T. (2014) Solution structure of calmodulin bound to the target Peptide of endothelial nitric oxide synthase phosphorylated at thr495. *Biochemistry 53*, 1241–1249.

(24) Zhang, M., and Vogel, H. J. (1994) Characterization of the calmodulin-binding domain of rat cerebellar nitric oxide synthase. *J. Biol. Chem. 269*, 981–985.

(25) Zhang, M., Yuan, T., Aramini, J. M., and Vogel, H. J. (1995) Interaction of calmodulin with its binding domain of rat cerebellar nitric oxide synthase: A multinuclear NMR study. *J. Biol. Chem. 270*, 20901–20907.

(26) Zoche, M., Bienert, M., Beyermann, M., and Koch, K. W. (1996) Distinct molecular recognition of calmodulin-binding sites in the neuronal and macrophage nitric oxide synthases: a surface plasmon resonance study. *Biochemistry 35*, 8742–8747.

(27) Piazza, M., Guillemette, J. G., and Dieckmann, T. (2015) Dynamics of nitric oxide synthase–calmodulin interactions at physiological calcium concentrations. *Biochemistry 54*, 1989–2000.

(28) Spratt, D. E., Newman, E., Mosher, J., Ghosh, D. K., Salerno, J. C., and Guillemette, J. G. (2006) Binding and activation of nitric oxide synthase isozymes by calmodulin EF hand pairs. *FEBS J. 273*, 1759–1771.

(29) Keller, R. L. J. (2005) Optimizing the process of nuclear magnetic resonance spectrum analysis and computer aided resonance assignment. Swiss Federal Institue of Technology Zurich.

(30) Grzesiek, S., and Bax, A. (1992) An efficient experiment for sequential backbone assignment of medium-sized isotopically enriched proteins. *J. Magn. Reson. 99*, 201–207.

(31) Grzesiek, S., and Bax, A. (1992) Correlating backbone amide and side chain resonances in larger proteins by multiple relayed triple resonance NMR. *J. Am. Chem. Soc. 114*, 6291–6293.

(32) Muhandiram, D. R., and Kay, L. E. (1994) Gradient-enhanced triple-resonance 3-dimensional NMR experiments with improved sensitivity. *J. Magn. Reson. 103*, 203–216.

(33) Ikura, M., Kay, L. E., and Bax, A. (1990) A novel approach for sequential assignment of 1H, 13C, and 15N spectra of proteins: heteronuclear triple-resonance three-dimensional NMR spectroscopy. Application to calmodulin. *Biochemistry 29*, 4659–4567.

(34) Ikura, M., and Bax, A. (1992) Isotope-filtered 2D NMR of a protein-peptide complex study of a skeletal muscle MLCK fragment bound to calmodulin. *J. Am. Chem. Soc.* 2433–2440.

(35) Clore, G. M., and Gronenborn, A. M. (1991) Applications of three- and four-dimensional

heteronuclear NMR spectroscopy to protein structure determination. *Prog. Nucl. Magn. Reson. Spectrosc. 23*, 43–92.

(36) Fesik, S. W., and Zuiderweg, E. R. P. (1990) Heteronuclear three-dimensional NMR spectroscopy of isotopically labelled biological macromolecules. *Quart. Rev. Biophys 23*, 97–131.

(37) Brunger, A. T., Adams, P. D., Clore, G. M., Delano, W. L., Gros, P., Grosse-kunstleve, R. W., Jiang, J., Kuszewski, J., Nilges, M., Pannu, N. S., Read, R. J., Rice, L. M., Simonson, T., and Gregory, L. (1998) Crystallography & NMR system : A new software suite for macromolecular structure determination. *Acta Cryst. D54*, 905–921.

(38) Aoyagi, M., Arvai, A. S., Tainer, J. A., and Getzoff, E. D. (2003) Structural basis for endothelial nitric oxide synthase binding to calmodulin. *EMBO J. 22*, 766–775.

(39) Xia, C., Misra, I., Iyanagi, T., and Kim, J.-J. P. (2009) Regulation of interdomain interactions by calmodulin in inducible nitric-oxide synthase. *J. Biol. Chem. 284*, 30708–30717.

(40) Chen, P. F., and Wu, K. K. (2000) Characterization of the roles of the 594-645 region in human endothelial nitric-oxide synthase in regulating calmodulin binding and electron transfer. *J. Biol. Chem. 275*, 13155–13163.

(41) Chen, P. F., and Wu, K. K. (2003) Structural elements contribute to the calcium/calmodulin dependence on enzyme activation in human Endothelial nitric-oxide Synthase. *J. Biol. Chem. 278*, 52392–52400.

(42) Knudsen, G. M., Nishida, C. R., Mooney, S. D., and Ortiz de Montellano, P. R. (2003) Nitric-oxide synthase (NOS) reductase domain models suggest a new control element in endothelial NOS that attenuates calmodulin-dependent activity. *J. Biol. Chem. 278*, 31814–31824.

(43) McMurry, J. L., Chrestensen, C. a, Scott, I. M., Lee, E. W., Rahn, A. M., Johansen, A. M., Forsberg, B. J., Harris, K. D., and Salerno, J. C. (2011) Rate, affinity and calcium dependence of nitric oxide synthase isoform binding to the primary physiological regulator calmodulin. *FEBS J. 278*, 4943–4954.

(44) Williams, D. H., Stephens, E., O'Brien, D. P., and Zhou, M. (2004) Understanding noncovalent interactions: ligand binding energy and catalytic efficiency from ligand-induced reductions in motion within receptors and enzymes. *Angew. Chem. Int. Ed. Engl. 43*, 6596–6616.

(45) Pervushin, K., Vamvaca, K., Vögeli, B., and Hilvert, D. (2007) Structure and dynamics of a molten globular enzyme. *Nat. Struct. Mol. Biol. 14*, 1202–1206.

(46) Ishima, R., and Torchia, D. A. (2000) Protein dynamics from NMR. *Nat. Struct. Biol. 7*, 740–743.

(47) Kay, L. E. (1998) Protein dynamics from NMR. *Biochem. Cell Biol. 76*, 145–152.

(48) Wand, A. J. (2001) Dynamic activation of protein function: a view emerging from NMR spectroscopy. *Nat. Struct. Biol. 8*, 926–931.

(49) Lipari, G., and Szabo, A. (1982) Model-free approach to the interpretation of nuclear magnetic resonance relaxation in macromolecules. 1. Theory and range of validity. *J. Am. Chem. Soc. 104*, 4546–4559.

(50) Spratt, D. E., Taiakina, V., and Guillemette, J. G. (2007) Calcium-deficient calmodulin binding and activation of neuronal and inducible nitric oxide synthases. *Biochim. Biophys. Acta 1774*, 1351–1358.

(51) Weissman, B. A., Jones, C. L., Liu, Q., and Gross, S. S. (2002) Activation and inactivation of neuronal nitric oxide synthase: Characterization of Ca2+-dependent [125I]Calmodulin binding. *Eur. J. Pharmacol. 435*, 9–18.

(52) Wu, G., Berka, V., and Tsai, A.-L. (2011) Binding kinetics of calmodulin with target peptides of three nitric oxide synthase isozymes. *J. Inorg. Biochem. 105*, 1226–1237.

(53) Venema, R. C., Sayegh, H. S., Kent, J. D., and Harrison, D. G. (1996) Identification, characterization,

and comparison of the calmodulin-binding domains of the endothelial and inducible nitric oxide synthases. *J. Biol. Chem. 271*, 6435–6440.

(54) Majava, V., Petoukhov, M. V, Hayashi, N., Pirila, P., Svergun, D. I., and Kursula, P. (2008) Interaction between the C-terminal region of human myelin basic protein and calmodulin: analysis of complex formation and solution structure. *BMC Struct. Biol. 8*, 10.

(55) Shen, Y., Lee, Y., Soelaiman, S., Bergson, P., Lu, D., Chen, A., and Beckingham, K. (2002) Physiological calcium concentrations regulate calmodulin binding and catalysis of adenylyl cyclase exotoxins. *EMBO J. 21*, 6721–6732.

(56) Guo, Q., Shen, Y., Lee, Y.-S., Gibbs, C. S., Mrksich, M., and Tang, W.-J. (2005) Structural basis for the interaction of Bordetella pertussis adenylyl cyclase toxin with calmodulin. *EMBO J. 24*, 3190–3201.

(57) Shukla, D., Peck, A., and Pande, V. S. (2016) Conformational heterogeneity of the calmodulin binding interface. *Nat. Commun. 7*, 10910.

Table 1. Statistics for the structural ensemble of the CaM−eNOS complex at 225 nM Ca^{2+}

	CaM-eNOS Complex			
NMR-derived distance and dihedral angle restraints				
	Calmodulin	eNOS peptide		CaM-eNOS complex
NOE constraints				
total	2836	86		37
dihedral angles from TALOS+	280	14		N/A
Total number of restraints		3253		
Structure statistics for the 20 lowest energy structures				
Mean deviation from ideal covalent geometry				
Bond lengths (Å)		0.010		
Bond angles (deg.)		1.2		
Average pairwise RMSD (Å) for all heavy atoms of the 20 lowest energy structures	All Residues	Ordered Residues[a]	C-lobe[b]	N-lobe[c]
Backbone Atoms	2.3	1.9	0.6	0.9
Heavy Atoms	2.6	2.2	1.1	1.4
Ramachandran statistics (%)				
Residues in most favored region		86.3		
Residues in additional allowed regions		13.2		
Residues in generously allowed region		0.4		
Residues in disallowed region		0.0		

[a] Ordered residue ranges: 4A-78A, 81A-134A, 137A-147A, 154B-161B
[b] C-lobe residues: 81A-148A
[c] N-lobe residues: 4A-74A

Table 2. k_{on} and k_{off} rate constants of eNOS target peptide to CaM at 225 nM Ca^{2+} and sat Ca^{2+}.

	k_{on} (10^4 $M^{-1}s^{-1}$)[a]	k_{off} (10^{-4} s^{-1})[a]	K_D (10^{-9} M)[a]
CaM-eNOS at sat Ca^{2+}	13.1 ± 4.8	3.5 ± 1.0	2.7 ± 0.2
CaM-eNOS at 225 nM Ca^{2+}	7.8 ± 0.5	8.3 ± 0.7	10.7 ± 0.3
CaM_{12}-eNOS at sat Ca^{2+}	11.2 ± 0.8	15.9 ± 4.4	14.4 ± 4.0
CaM_{12}-eNOS at 225 nM Ca^{2+}	5.1 ± 0.4	9.1 ± 0.7	18.0 ± 2.7
CaM_{34}-eNOS at sat Ca^{2+}[b]	5.8 ± 0.9	13.4 ± 0.3	22.7 ± 1.5

[a] Data was fit in TraceDrawer using a 1:1 binding interaction model (A+B ↔ AB) with standard deviation of three experiments.

[b] Binding of CaM_{34} to eNOS was very weak at 225 nM free Ca^{2+}.

FIGURE CAPTIONS

FIGURE 1. Solution structures of CaM bound to the eNOS CaM binding peptide at 225 nM Ca^{2+}. Superposition of the ensemble of the 20 lowest-energy calculated NMR solution structures of (a) CaM bound to eNOS peptide at 225 nM Ca^{2+} and (d) the previously determined solution structures of CaM bound to eNOS peptide at saturated Ca^{2+}. The superposition is aligned by the backbone atoms of the C-lobe of CaM. Backbone atom traces of CaM are colored dark blue, and the eNOS peptide colored light blue. Cartoon ribbon view of the average solution structure of the CaM− eNOS complex at (b) 225 nM Ca^{2+} and (e) saturated Ca^{2+}. Residues 1−40 of CaM (EF hand I) are colored red, residues 41−79 (EF hand II) purple, residues 80−114 (EF hand III) green, and residues 115−148 (EF hand IV) blue. The peptide is colored lighter blue. Calcium ions are colored green. CaM N and C termini are identified by N and C, while the peptide N and C termini are identified by N' and C'. Worm models of CaM-eNOS peptide complex at (c) 225 nM Ca^{2+} and (f) saturated Ca^{2+} illustrating their internal dynamics and amide H/D exchange data. The worm models were prepared using UCSF Chimera with the render by attribute function. The worm radius ranges from 0.25 (S^2 value of 1), to 4 (S^2 value of 0.4). Residues that display fast D_2O exchange rates are colored red on the ribbon structure. Residues that display intermediate D_2O exchange rates are colored light blue and residues that display slow D_2O exchange rates are colored blue. The bound peptide is colored black and shown in wire form.

FIGURE 2. Comparison of the solution structure of the CaM-eNOS peptide complex at 225 nM Ca^{2+} with the solution structures of saturated Ca^{2+} CaM-eNOS peptide complex and apoCaM. The solution structures of the CaM−eNOS peptide at 225 nM Ca^{2+} (dark colors) and at saturated Ca^{2+} (light colors) are aligned by superimposition of the backbone atoms of the C-lobes of CaM (a) viewed along the bound peptide from its N-terminus (N′) to its C-terminus (C′) and (b) rotated around the horizontal axis with the C-terminus of the bound peptide on the top. The solution structures of the CaM−eNOS peptide at 225 nM Ca^{2+} (dark colors) and apoCaM (light colors) are aligned by superimposition of the backbone atoms of the N-lobes of CaM (c) viewed along the bound peptide from its N-terminus (N′) to its C-terminus (C′)

and (d) rotated around the horizontal axis with the C-terminus of the bound peptide on the top. The color scheme for the EF hands is the same as that in Figure 1.

FIGURE 3. Solution structures of CaM bound to the eNOS CaM binding peptide at 225 nM Ca^{2+} showing sidechain residues of CaM interacting with side chains of the anchor residues of the eNOS peptide. (A) Cartoon ribbon view of the average solution structure of the CaM− eNOS complex at 225 nM Ca^{2+} showing sidechain residues of CaM interacting with side chains of the anchor residues of the eNOS peptide. The side chains are colored by the same color scheme as that in Figure 1. (B) Zoom in of the C-lobe of CaM showing sidechain residues of CaM interacting with side chains of the anchor residues of the N-terminus of the eNOS peptide (showing α-helical structure). (C) Zoom in of the N-lobe of CaM showing sidechain residues of CaM interacting with side chains of the anchor residues of the C-terminus of the eNOS peptide (showing random coil structure).

FIGURE 4. SPR sensorgrams of the binding of various CaM constructs onto immobilized eNOS peptide at saturating Ca^{2+} (0.1 mM $CaCl_2$) and 225 nM free Ca^{2+} on OpenSPR. Sensorgrams were recorded using increasing amounts of CaM (from 10 – 500 nM) in either the saturating Ca^{2+} (0.1 mM $CaCl_2$) or 225 nM free Ca^{2+} buffer running buffer during the association phase. Dissociation of the CaM-eNOS complex was observed by running either saturating Ca^{2+} (0.1 mM $CaCl_2$) or 225 nM free Ca^{2+} buffer without CaM over the flow cell.

FIGURE 5. K_D versus k_{off} for various CaM constructs and eNOS peptides at saturating Ca^{2+} (0.1 mM $CaCl_2$) and 225 nM free Ca^{2+}.

FIGURES

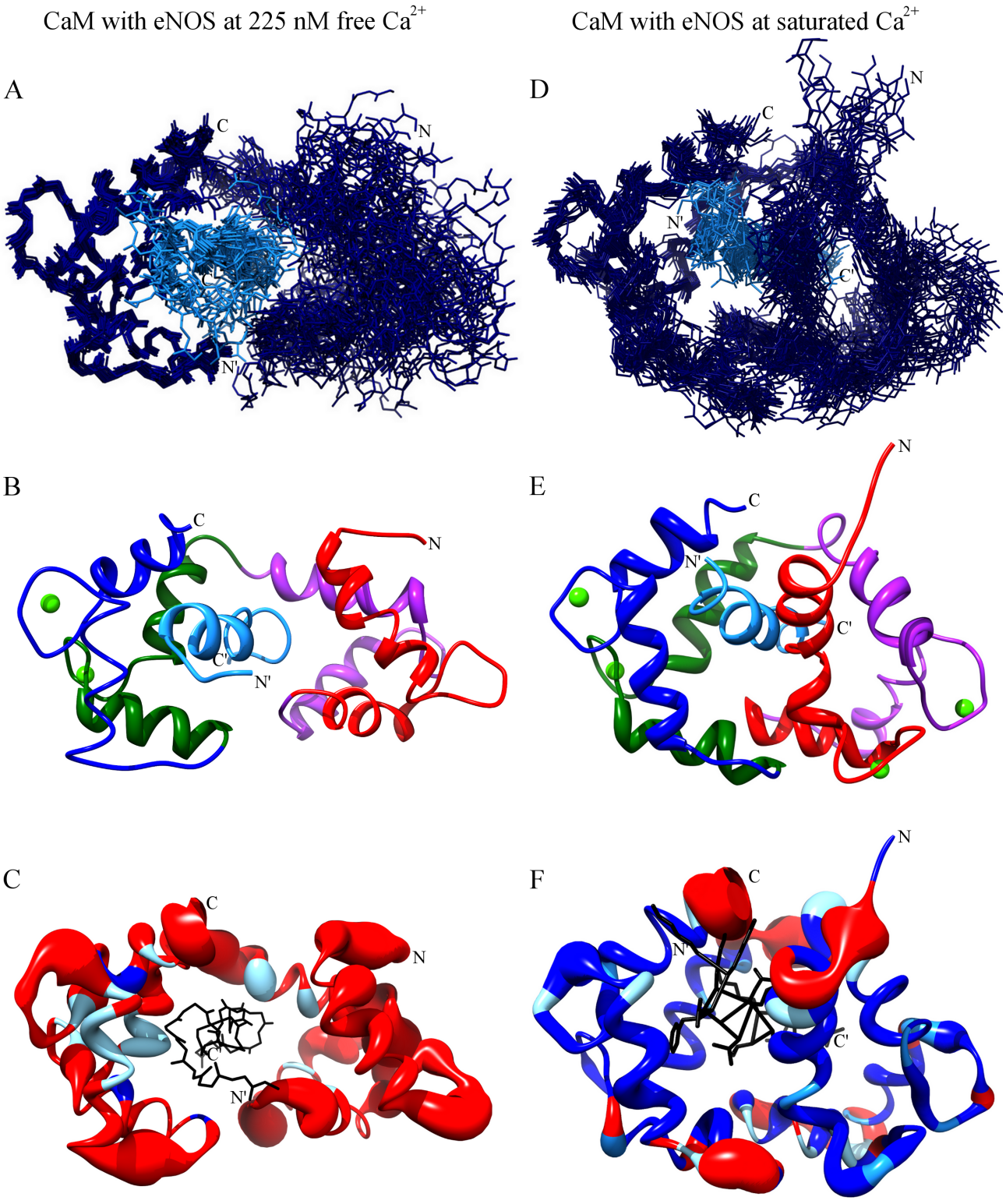

Figure 1

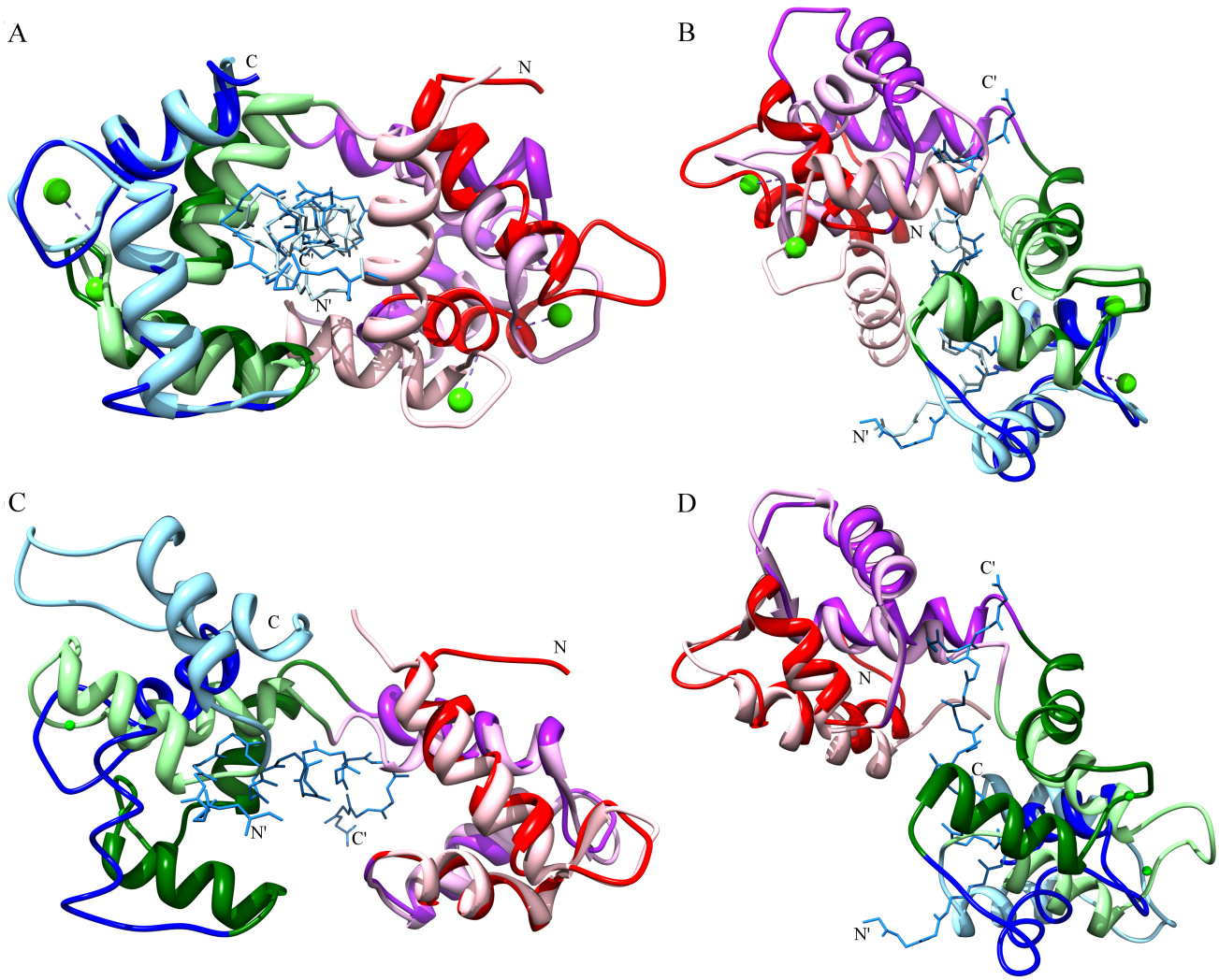

Figure 2

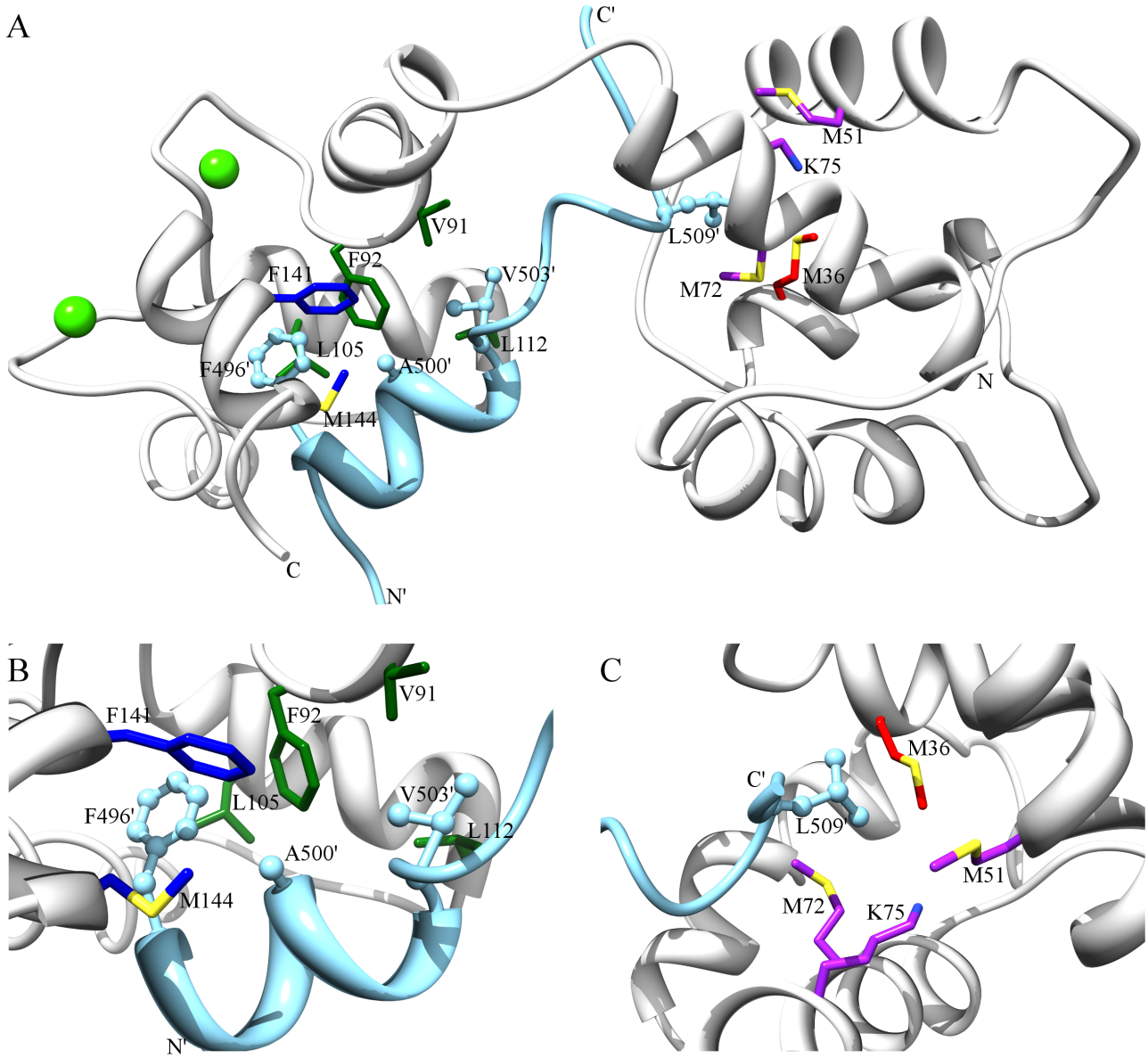
A
C'
M51
K75
V91
L509'
F92
F141
V503'
M72
M36
L105
L112
F496'
A500'
N
M144
C
N'
B
F141
V91
F92
V503'
F496'
L105
L112
A500'
M144
N'
C
M36
C'
L509'
M51
M72
K75

Figure 3

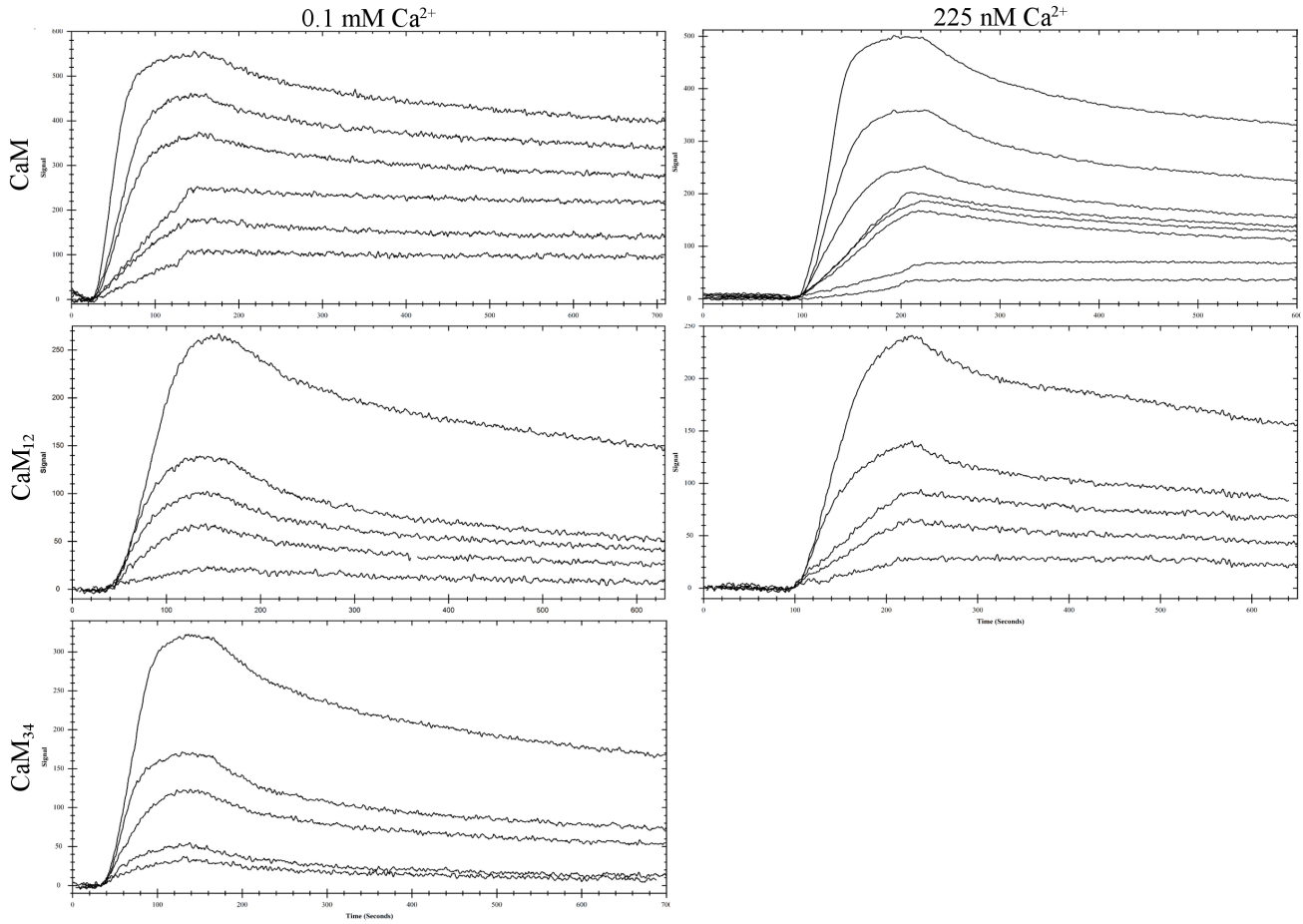

Figure 4

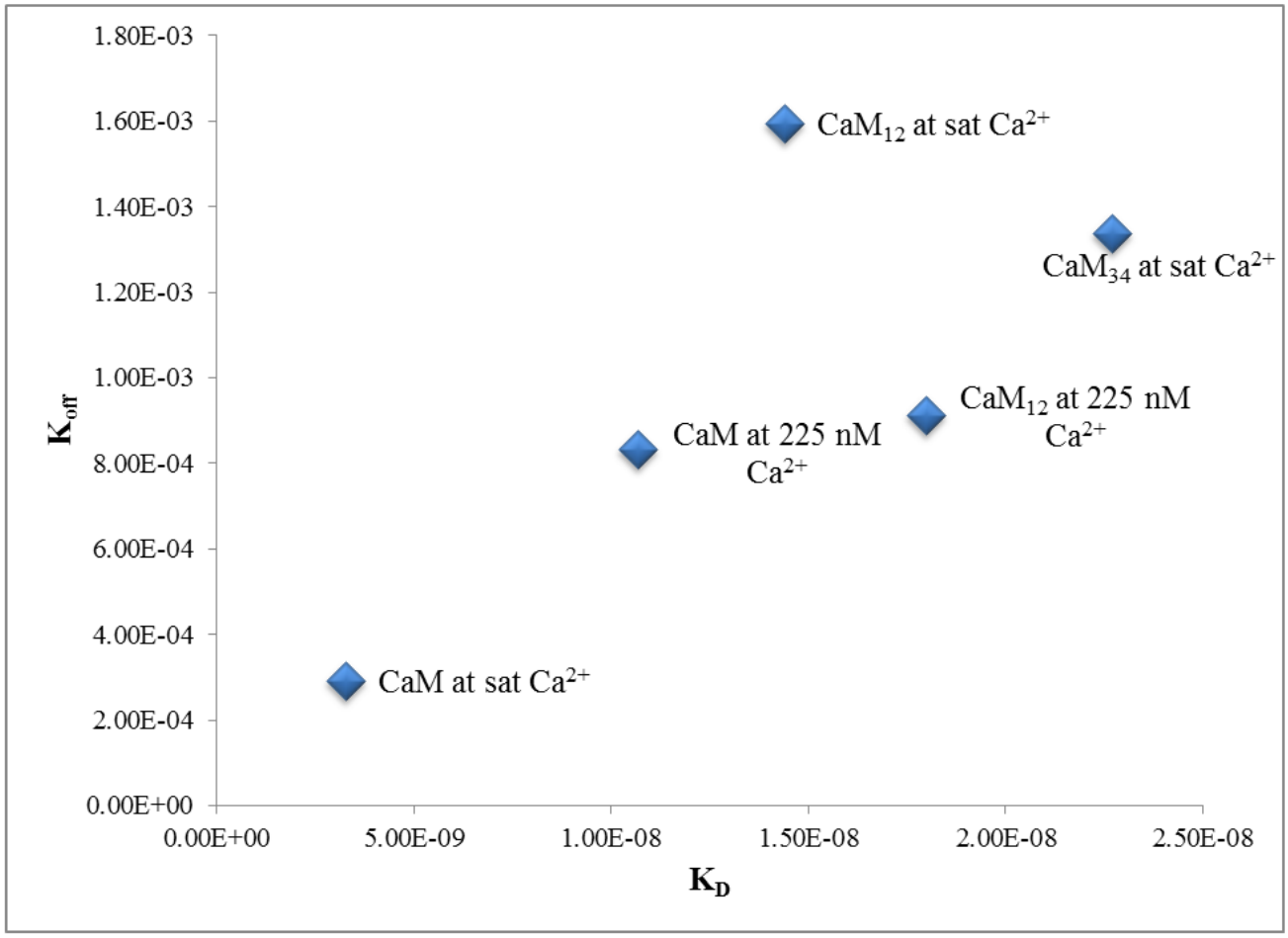
1.80E-03
1.60E-03
1.40E-03
1.20E-03
1.00E-03
8.00E-04
6.00E-04
4.00E-04
2.00E-04
0.00E+00
K_{off}
0.00E+00
5.00E-09
1.00E-08
1.50E-08
2.00E-08
2.50E-08
K_D
CaM_{12} at sat Ca^{2+}
CaM_{34} at sat Ca^{2+}
CaM_{12} at 225 nM Ca^{2+}
CaM at 225 nM Ca^{2+}
CaM at sat Ca^{2+}

Figure 5

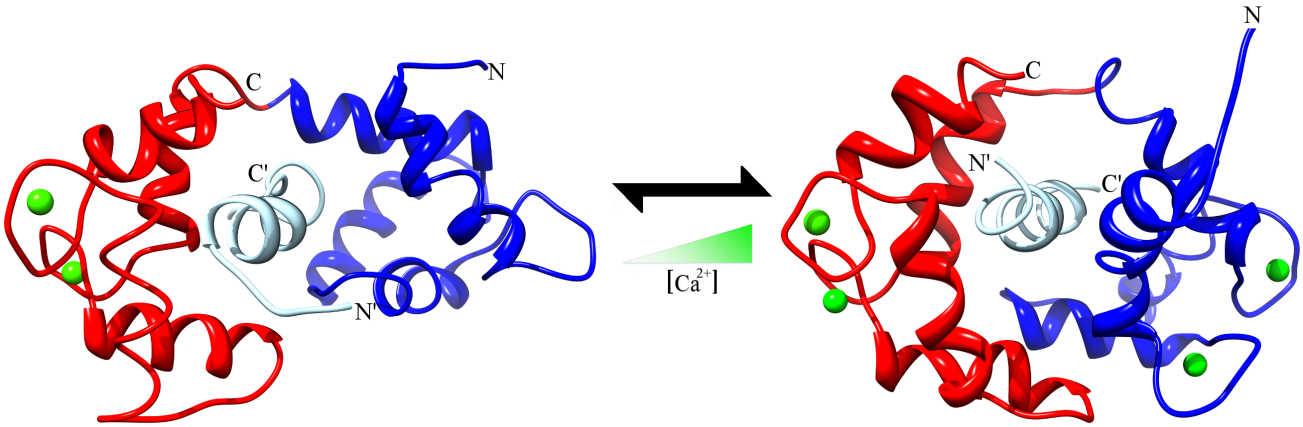

Graphic for Table of Contents